Environmental Pollution 348 (2024) 123823

Contents lists available at ScienceDirect

Environmental Pollution

journal homepage: www.elsevier.com/locate/envpol

Harmful effects of true-to-life nanoplastics derived from PET water bottles in human alveolar macrophages.☆

Alireza Tavakolpournegari [a], Aliro Villacorta [a,b], Michelle Morataya-Reyes [a], Jéssica Arribas Arranz [a], Gooya Banaei [a], Susana Pastor [a], Antonia Velázquez [a], Ricard Marcos [a,*], Alba Hernández [a], Balasubramanyam Annangi [a]

[a] Group of Mutagenesis, Department of Genetics and Microbiology, Faculty of Biosciences, Universitat Autònoma de Barcelona, Cerdanyola del Vallès, Barcelona, Spain
[b] Facultad de Recursos Naturales Renovables, Universidad Arturo Prat, Iquique, Chile

ARTICLE INFO

Keywords:
PET
MH-S cells
ROS
Mitochondrial membrane potential
Macrophage polarization

ABSTRACT

The increasing presence of secondary micro/nanoplastics (MNPLs) in the environment requires knowing if they represent a real health concern. To such end, an important point is to test representative MNPLs such as the denominated true-to-life MNPLs, resulting from the degradation of plastic goods in lab conditions. In this study, we have used polyethylene terephthalate (PET) NPLs resulting from the degradation of PET water bottles. Since inhalation is an important exposure route to environmental MNPLS, we have used mouse alveolar macrophages (MH-S) as a target cell, and the study focused only on the cells that have internalized them. This type of approach is novel as it may capture the realistic adverse effects of PETNPLs only in the internalized cells, thereby mitigating any biases while assessing the risk of these MNPLs. Furthermore, the study utilized a set of biomarkers including intracellular reactive oxygen species (ROS) levels, variations on the mitochondrial membrane potential values, and the macrophage polarization to M1 (pro-inflammatory response) and M2 (anti-proinflammatory response) as possible cellular effects due to PETNPLs in only the cells that internalized PETNPLs. After exposures lasting for 3 and 24 h to a range of concentrations (0, 25, 50, and 100 μg/mL) the results indicate that no toxicity was induced despite the 100% internalization observed at the highest concentration. Significant intracellular levels of ROS were observed, mainly at exposures lasting for 24 h, in an indirect concentration-effect relationship. Interestingly, a reduction in the mitochondrial membrane potential was observed, but only at exposures lasting for 24 h, but without a clear concentration-effect relationship. Finally, PETNPL exposure shows a significant polarization from M0 to M1 and M2 subtypes. Polarization to M1 (pro-inflammatory stage) was more marked and occurred at both exposure times. Polarization to M2 (anti-inflammatory stage) was only observed after exposures lasting for 24 h. Due to the relevance of the described biomarkers, our results underscore the need for further research, to better understand the health implications associated with MNPL exposure.

1. Introduction

Plastic pollution is an important environmental concern due to the ever-increasing utilization of plastic products in each sphere of human life. The presence of large amounts of plastic materials in nature would result in both physical and chemical or biological degradation into smaller particles such as micro and nano-plastics (MNPLs). Subsequently, they are released into the environment eventually reaching different types of ecosystems and making them a global environmental concern (Rubio et al., 2020; Gigault et al., 2021; Kumar et al., 2022). Due to that, there has been a good scope of MNPLs presence in marine food web because of their ingestion, subsequently giving rise to the trophic transfer of MNPLs to humans with potential human health implications (Carbery et al., 2018). In agreement, a few recent studies evaluated the potential trophic transfer of nanoplastics in marine organisms *via* a three-step food chain as well as reaching humans through trophic transfer. It was shown that exposure of microalgae (*Dunaliella salina*) to amine-modified nanopolystyrene was transferred to small

☆ This paper has been recommended for acceptance by Maria Cristina Fossi.

* Corresponding author. Group of Mutagenesis, Department of Genetics and Microbiology, Faculty of Biosciences, Universitat Autònoma de Barcelona, Campus of Bellaterra, 08193, Cerdanyola del Vallès, Barcelona, Spain.
E-mail address: ricard.marcos@uab.cat (R. Marcos).

https://doi.org/10.1016/j.envpol.2024.123823
Received 21 December 2023; Received in revised form 8 February 2024; Accepted 18 March 2024
Available online 19 March 2024

crustaceans (*Artemia franciscana)*, and to fish (*Larimichthys polyactis)*, eventually reaching higher trophic level organisms such as humans by the food chain. This resulted in the inhibition of digestive enzyme activity (α-amylase) in humans (Kim et al., 2022). Similarly, a food web accumulation modeling to simulate a lake ecosystem revealed the accumulation of microplastics (MPLs) *via the* food web in marine organisms and higher trophic levels like humans prone to consumption of MPs contaminated seafood (Bhutto et al., 2023). Additionally, human exposure to MNPLs to humans could come from different plastic sources utilized commercially, they could reach the human system *via* various routes of exposure such as oral, inhalation, and dermal (Lim et al., 2021).

Potentially, the inhalation route of exposure to atmospheric MNPLs in humans could trigger oxidative stress and inflammation in lung tissue due to their translocation to the lungs, where the immune responses involving inflammatory cells like macrophages, in particular, human alveolar macrophages of the pulmonary system would be in direct contact and could internalize them *via* phagocytosis, thereby playing a crucial role in the immune defense of the human body. However, the functional aspects of macrophages could be affected if the exposure to MNPLs lasts for a long period (Allard et al., 2018; Chen et al., 2022; Jenner et al., 2022). Thus, the importance of investigating the implications of MNPLs in human health specifically focusing on immune response at cellular and tissue levels is inevitable (Le et al., 2023). The polymeric plastics that are found in the environment are made up of different chemical polymers like polyethylene (PE), polyvinyl chloride (PVC), polystyrene (PS), polypropylene (PP), and polyethylene terephthalate (PET) (Tursi et al., 2022). Among these, PET is the most widely used plastic material for manufacturing plastic bottles e.g., water storage and transport bottles (Villacorta et al., 2022). Hence, their fate in the atmosphere and their possibility to reach the human body, including the respiratory system, is a matter of growing environmental and human health concern (Annangi et al., 2023). Accordingly, several studies have utilized macrophages of different tissular origin to show the potential of MNPLs in eliciting inflammatory responses after their exposure under *in vitro* conditions (Collin-Faure et al., 2022; Wang et al., 2023). Thus, MNPLs released from plastic food packaging (mainly polypropylene and PET) were easily engulfed by alveolar macrophage RAW264.7 cells inducing inflammation (MPLs) and suppressing the lysosomal activity (NPLs) (Deng et al., 2022). In addition, lipid metabolism alterations in human M1 macrophages exposed to polypropylene and polyvinyl chloride NPLs were observed, affecting oxidative stress and phagocytosis mechanisms (Zingaro et al., 2023). In a most recent finding (Washihira et al., 2023), PETNPLs were able to trigger an immune response as there was a significant increase in inflammatory cytokine secretion after their treatment of human macrophages. Nevertheless, while the mentioned studies did focus on the immunotoxic effects of MNPLs in general, none of them had considered the cellular effects of PETNPLs in subpopulations of macrophages with and without MNPL internalization. Moreover, there is a lack of comprehensive studies showing the subtle toxic effects in sorted populations of macrophages with PETNPLs among the total exposed macrophage population. Hence, we investigated the specific hazard effects of these nanoplastics by sorting and monitoring only the macrophages containing PETNPLs, we regarded them as a target population among the total exposed cells.

In this study, mouse alveolar macrophages (MH-S cells) were used to assess the potential adverse effects associated with true-to-life PETNPL exposure in only the cells that internalized them, as compared to the subpopulation without cellular internalization. This study considered different concentrations of PETNPLs. Furthermore, we sorted the cells specifically based on the PETNPLs internalization using the cell sorter technique, later the sorted cells with PETNPLs were studied for their cellular effects such as the increase in reactive oxygen species (ROS), loss of mitochondrial membrane potential, as well as the macrophagic polarization into important subtypes. It must be remembered that to fulfill their functional roles, macrophages undergo polarization to the classically (M1) and alternatively activated (M2) subtypes; M1 macrophages are capable of pro-inflammatory responses, and M2 macrophages of anti-proinflammatory responses. Thus, determining if MNPLs can modulate such polarizations is of great relevance. The selected cells are regarded as model cells for toxicological and immunological studies, including those induced by MNPLs (Delaney et al., 2023). Several studies have used macrophages to show the *in vitro* potential of MNPLs to cause inflammatory responses, polarization of macrophages into different sub-types, DNA damage, as well as loss of mitochondrial membrane potential (Pulvirenti et al., 2022; Koner et al., 2023; Wang et al., 2023).

In summary, the hypothesis of the study was to understand whether cell sorting based on the internalized PETNPLs could aid in estimating the subtle or sub-toxic effects in the sorted cells otherwise these changes may go unnoticed as compared to the total unsorted exposed population of cells. For that, our main aim was to assess the cellular changes observed in those cells that internalized PETNPLs, in comparison with the total exposed population, at different concentrations and time intervals.

2. Materials and methods

2.1. Obtention, labeling, and characterization of PETNPLs

Laboratory-manufactured PETNPLs were prepared using the method described by Villacorta et al. (2022). In brief, commercially available PET plastic water bottles underwent sanding using a diamond rotary burr. The resulting powder was sieved through a 0.20 mm mesh and subsequently, 4 g of this material were combined with 40 mL of 90% trifluoroacetic acid (TFA) preheated to 50 °C. The mixture was stirred continuously at 200 rpm on a heated stirring plate (Heidolph Instruments GmbH & Co. KG, Schwabach, Germany) for 2 h, followed by agitation at room temperature overnight, and 40 mL of TFA 20% was added to the suspension. After the removal of large agglomerates/aggregates, the remaining volume was divided into glass tubes and centrifuged at 2500 relative centrifugal force (RCF) for 1 h. The resulting pellet was resuspended in 400 mL of 0.50% sodium dodecyl sulfate (SDS), subjected to sonication, and then transferred to 250 mL beakers and subjected to sonication on 9/9 s intervals of sonication and breaks for 2 min, and then transferred to a graded cylinder, allowing the larger fraction to settle for 1 h. The top 100 mL from each cylinder were collected and washed twice with water and pure ethanol, and the resulting pellet was resuspended in Milli-Q water at the desired concentrations. After sonication, the suspension was stored at −80 °C, and ready-to-use aliquots were prepared by using the Nanogenotox protocol (Nanogenotox project, 2011).

The labeling of PETNPLs with a commercial fluorescent dye was accomplished by following the adapted protocol previously published for both commercial (Tavakolpournegari et al., 2023) and lab-made plastics (Annangi et al., 2023). Such protocol was based on the studies previously reported (Karakolis et al., 2019; Nguyen and Tufenkji, 2022). In summary, a working solution comprising 1 mL of PETNPLs at a concentration of 5 mg/mL was introduced into a 1.5 mL tube containing 0.01 g of iDye Poly Pink (hereafter referred to as iDye). The resultant mixture was vortexed and then incubated at 70 °C for 1 h, later the mixture was allowed to cool down to room temperature and transferred to a falcon tube containing 9 mL of Milli-Q water. The resulting 10 mL of solution was centrifuged at 4000 rpm and filtered to eliminate the excess iDye. The PETNPLs labeled with iDye were subsequently resuspended in 10 mL of Milli-Q water, subjected to centrifugation at 4000 rpm twice, and finally resuspended in 1 mL of Milli-Q water. Thus, labeled iDye-PETNPLs were stored in light-protected conditions at 4 °C.

To evaluate the characteristics of the generated PETNPLs, scanning electron microscopy was performed on a Zeiss Merlin scanning electron microscopy (SEM) system (SEM Zeiss Merlin, Zeiss, Oberkochen,

Germany), following the protocol previously reported (Villacorta et al., 2023). Briefly, a working solution of the particle suspension at a concentration of 100 μg/mL was prepared. A 20 μL drop was placed on a silicon holder of 5 × 5 mm (Ted Pella, INC. Altadena California) and let dry covered under the laminar hood. For better contrast, samples were sputter-coated with a gold/palladium thin layer in an Emitech K550X from Quorum (Laughton, East Sussex, United Kingdom) as described (Domenech et al., 2020). Particles were analyzed by taking micrographs from random fields and counting a minimum of 1000 particles. To evaluate the hydrodynamic behavior of a solid colloidal spherical structure corresponding to our sample, the hydrodynamic behavior of the particle suspension was measured on water and on RPMI-supplemented media previously described on a Zetasizer® Ultra Red from Malvern Panalytical (Cambridge, United Kingdom). A collection angle of 174.7° was used for DLS. The refraction index of PET used for this study was 1.57 while for water was 1.33 and 1.34 for supplemented RPMI. The Z-potential was also evaluated using a DTS 1070 cuvette. For determining the lambda emission of our particle suspensions, particles were allowed to aggregate on a glass slide before observation. Slides were washed with methanol under a BSL2 laminar flow cabin and once the methanol evaporated a 20 μL drop of iDyePET-NPLs was deposited on the surface and a coverslip was immediately placed. A minimum of 15 min prior to observation was waited before the samples were studied on a Zeiss LSM 980 confocal system (Zeiss, Oberkochen, Germany). The selected excitation wavelength was 561 nm, and the emission was collected from 580 to 770 nm. For all cases, the data was arranged and analyzed using GraphPad prism 8.0 (GraphPad, San Diego, CA) and images were prepared using ImageJ software 1.8.0_172.

2.2. Cell culture

The mouse alveolar macrophage cell line (MH-S) utilized in this study was a generous gift by Dr. José Domínguez from the Innovation in Respiratory Infections and Tuberculosis Diagnosis Group at the Institut d'Investigació en Ciències de la Salut Germans Trias i Pujol, Barcelona, Spain. The MH-S cells were cultured in RPMI-1640 medium (supplied by Biowest, lnc.), which was enriched with 10% fetal bovine serum, 1% penicillin/streptomycin, and 2.5 μg/mL of Plasmocin. The cells were incubated at a temperature of 37 °C in an environment containing 5% CO_2. The cell culture medium was changed with fresh pre-warmed medium every 2–3 days.

2.3. MH-S cells treatment with PETNPLs

Cells were treated with various concentrations of PETNPLs suspended in RPMI-1640 medium to investigate their potential toxic effects. Different cell densities were seeded for each type of assay, as further detailed in the corresponding section. After seeding, the cells were exposed to different concentrations of PETNPLs (0, 25, 50, and 100 μg/mL) for 3 and 24 h, based on the endpoints of the study. We regarded these concentrations as the first starting point to know any significant decreases in cell viability. This would reveal the sub-toxic concentrations at which the cells would withstand the PETNPLs-induced cell death, thereby subtle changes or sub-toxic cellular functions could be investigated. A similar range of different concentrations of MNPLs was selected by Yang et al. (2021) to assess the human lung response after their exposure. Furthermore, the shorter duration of exposures was based on the cellular internalization of PETNPLs in macrophages, at these treatment time points, PETNPLs may potentiate acute cellular effects, particularly in the sorted cells with PETNPLs. Taken together, the evaluation of the adverse effects of PETNPLs in the sorted cells was acute.

2.4. Cell sorting and isolation of iDye-PETNPLs internalized cells

For the specific objective of visualizing iDye-PETNPLs internalization, when using confocal microscopy, exposed cells were sorted using the cell sorter (FACSJazz cell sorter, Becton Dickinson, USA). Both, cells with internalized PETNPLs (positive) and without (negative) were sorted and suspended in RPMI-1640 medium based on the fluorescence intensity of iDye-PETNPLs at 585 nm emission (10,000 events recorded and gated using BD FACJazz software). To confirm the internalization of PETNPLs in sorted cells, confocal microscopy was used. For this purpose, a total of 80,000 sorted cells were seeded in microwell dishes with glass bottoms (MatTek, Ashland, OR, USA) and immediately assessed by confocal microscopy. The nuclei and cell membrane were stained with Hoechst dye (ThermoFisher Scientific, Carlsbad, CA, USA) at a dilution of 1:500 and Cellmask™ Deep Red plasma (ThermoFisher Scientific, Carlsbad, CA, USA) at a dilution of 1:500, respectively. This staining process takes place for 15 min at room temperature. To visualize the iDye-PETNPLs within cells the emission wavelength of 585 nm was used. It was achieved using a Leica TCS SP5 confocal microscope. Multiple fields were randomly chosen from each sample. The acquired images were then processed utilizing ImageJ software with the Fiji extension.

2.5. Cell viability

MH-S cells were collected by centrifugation (100 rcf for 7 min) and resuspended in RPMI-1640 medium to reach the density of 2.5×10^5 cells/mL and then seeded in a 12-well plate. Exposure to PETNPLs lasts for 24 h with a range of concentrations (0, 25, 50, and 100 μg/mL. After exposure, the cells were diluted with Isoton solution (1:200) and counted with ZTM series Coulter counter (Beckman Counter lnc., CA). The derived percentage values were calculated as the mean count of cells for each treatment, relative to the values from the untreated control cells.

2.6. Intracellular ROS induction assessment

The ability of PETNPLs to produce reactive oxygen species (ROS) in MH-S cells was assessed by using the DCFH-DA (2′,7′-dichlorodihydrofluorescein diacetate) method using flow cytometry. To be sure that ROS was measured only in the cells internalizing PETNPL, the MH-S cells were exposed to the iDye-PETNPLs (0, 25, 50, and 100 μg/mL) for 3 and 24 h. After exposure, the cells were detached by using trypsin (0.05%), centrifuged at 200 rcf for 10 min, pelleted, and then suspended in 10 μM of DCFH-DA at 37 °C for 30 min. The exposed cells were washed with PBS and analyzed by flow cytometry (CytoFlex, Beckman Coulter, USA). Hydrogen peroxide (H_2O_2, 1 mM) was used as a positive control. Cells containing PETNPLs were gated based on the fluorescent intensity of iDye-PETNPLs at 585 nm emission, and the fluorescent intensity of DCFH-DA was assessed in the gated population at 530 nm emission. 10,000 cells per sample were scored and analyzed with the Cytexpert software.

2.7. Measurement of mitochondrial membrane potential

The loss of mitochondrial membrane potential (MMP) in MH-S cells due to PETNL exposure was measured by using the TMRM Mitoprob assay in the gated cells using flow cytometry. Cells were exposed to iDye-PETNPLs (0, 25, 50, and 100 μg/mL) for 3 and 24 h. After exposure, cells were pelleted and treated with 20 nM of TMRM prob for 30 min at 37 °C. The exposed cells were washed with PBS and analyzed by flow cytometry (CytoFlex, Beckman Coulter, USA). Carbonyl cyanide m-chlorophenyl hydrazone (CCCP, 5 μM) was used as a positive control and incubated for 5 min at 37 °C. By using flow cytometry, those cells containing PETNPLs were gated based on the fluorescent intensity of the iDye-staining with the excitation-emission of 561–630 nm respectively, and the fluorescent intensity of TMRM prob was also assessed in the

gated population with the excitation-emission of 488–560 nm respectively. About 10,000 cells per sample were scored and analyzed with Cytexpert software.

2.8. Macrophage polarization assay by flow cytometry (FC)

One of the important responses of the macrophages, as immune cells, to the environmental agents is their polarization from M0 to M1 (pro-inflammatory subtype) and M2 (anti-inflammatory subtype) which would indicate their sensitivity to external stimuli (Fuchs et al., 2016). Accordingly, determining if PETNPLs trigger macrophagic polarization is something to be known. For that, macrophage polarization assessment was carried out by using FITC fluorescent conjugated anti-CD86 and anti-CD163 monoclonal antibodies (Thermofisher Scientific, USA) to detect M1 and M2 polarized macrophages, respectively. Cells were exposed to iDye-PETNPLs (0, 25, 50, and 100 μg/mL) for 3 and 24 h. After exposure, cells were pelleted and treated with concentrations of 500 μg/mL and 250 μg/mL of CD86 and CD163, respectively, for 30 min at 4 °C. The exposed cells were washed with PBS and analyzed by flow cytometry (CytoFlex, Beckman Coulter, USA). LPS at the concentration of 10 μg/mL was used as a positive control by treating the cells for 24 h. By cytometry, cells containing PETNPLs were gated based on the fluorescent intensity of the iDye-stain with the excitation-emission of 561–630. The fluorescent intensity of antibodies was evaluated in the gated population with the excitation-emission of 488–520 nm for CD86 and the excitation-emission of 405–436 nm for CD163 (in separate experiments for each antibody). The amount of 10,000 cells per sample was scored and analyzed by using the Cytexpert software.

2.9. Macrophage polarization assay by confocal microscopy

To complement flow cytometry data, macrophage polarization was assessed by using confocal microscopy. To proceed, cells were seeded in a 6-well glass bottom dish with a density of 80,000 cells/well and treated with iDye-PETNPLs for 24 h (100 μg/mL). After exposure, cells were washed thrice with cold PBS and fixed with 4% paraformaldehyde incubated at 4 °C for 10 min. Later, cells were incubated with a blocking buffer (1% bovine serum albumin) for 45 min at 4 °C. Following, anti-CD86 and anti-CD163 antibodies were added and incubated for 2 h at room temperature. Finally, cells were washed twice with PBS, and phalloidin (0.5%) was added to the cells to stain the cytoskeleton. The excess stain was removed by rinsing with PBS. Nuclei were stained with Hoechst dye (ThermoFisher Scientific, Carlsbad, CA, USA) at a dilution of 1:500 for 15 min at room temperature. To visualize iDye-PETNPLs, CD86, CD163, and phalloidin within the cells, the emission wavelengths of 585, 520, 436, and 488 nm were used, respectively. This visualization was achieved using a Zeiss LSM 980 confocal microscope. Multiple fields were randomly chosen from each sample. The acquired images were then processed utilizing ImageJ software with the Fiji extension.

2.10. Statistical analysis

Data, represented as the mean ± SEM values, were derived from three independent experiments, each of which was conducted by duplicate. For the statistical evaluation, a two-way ANOVA with Turkey's multiple comparison tests was used, except where specifically noted otherwise. Significance levels were established as follows: $*p \leq 0.05$, $**p \leq 0.01$, and $***p \leq 0.001$. Data analysis was conducted using GraphPad prism 8.0 (GraphPad, San Diego, CA).

3. Results and discussion

3.1. Characterization of PETNPLs and visualization of labeled PETNPLs

The size distribution and shape of PET nanoparticles in suspension were assessed using scanning electron microscopy for the dry state, and a Zetasizer device for the hydrodynamic behavior. The micrograph in Fig. 1a shows differences in particle morphology as well as in the polydispersity nature of the sample on water dispersion. The calculated average size of the particles in the dry state, as informed in Fig. 1b–is slightly smaller (163.01 nm) than the size informed by DLS for water dispersion (292.00 nm), while the PDI value for both cases is never smaller than 3.9. This average size value (Z-average) is greater when RPMI is used for particle dispersion (1140 nm), which is a clear indicator of the presence of aggregates. The comparison of water dispersion and RPMI dispersion can be observed in Fig. 1c. One of the principal reasons for this increase in the hydrodynamic behavior may be the irregular shape of the particles, which may increase the contact surface interactions between particles and media components. The 0.3% of big aggregates detected by SEM (over 1 μm) could be highly represented due to the scattering effects or the increase of the suspension fraction behaving in this manner. The reported data are well represented by the correlation curves of the different measurements carried out, as depicted in Fig. 1d. These values, which could be interpreted as a huge increase in the Z-average values, shifting from 292 nm to more than 1 μm agree with the shift observed for the Z-potential where a significant decrease on the absolute value from −26 to −8 is observed, indicating that the suspension is more prone to form aggregates when the dispersion is made using supplemented culture media.

Regarding the labeled PETNPLs, the visualization was done by confocal microscopy, as observed in Fig. 1e, where the labeled PETNPLs are observed as green spots resulting from the presence of big particle clusters formed on the glass slide. Fig. 1f shows the emission spectra of these stained particles which peak from 610 to 620 nm. That peak emission agrees with the expected emission spectra of iDye which moves from 585 to 700 nm. In addition, no background fluorescence was observed indicating a lack of leaching, which all together indicates the suitability of the stained particles as a suitable model.

3.2. PETNPLs uptake detection by confocal microscopy, using sorted cells

Cell sorting by flow cytometry has been classically used to select and isolate a desired population of cells, from an heterogenous culture. In our case, we used iDye-labeled PETNPL to detect light signals in specific wavelengths emitted by those target cells internalizing labeled PETNPLs. This cell-sorting approach has been used to isolate different cell types internalizing or not fluorescent nanoparticles (Latroche et al., 2018; Ciaglia et al., 2019).

The identification and isolation of cells containing PETNPLs were carried out by assessing the fluorescent intensity of the particles. Subsequently, those cells containing internalized PETNPLs were sorted and collected from the live cell population, previously exposed to three different concentrations (25, 50, and 100 μg/mL) of iDye-labeled PETNPL. The percentage of cells that internalized PETNPLs, from the overall exposed cell population, is indicated in Supplementary Fig. S1. The internalization levels show a direct relationship with exposure concentrations where 100 percent of the cells exposed to the concentration of 100 μg/mL internalized PETNPLs. To confirm that all the positive gated cells carried internalized PETNPLs, positive cell sorting was carried out and confocal microscopy was applied to the selected cells. As observed in Fig. 2, the obtained confocal images confirmed that 100% of the sorted cells possessed intracellular iDye-PETNPLs. Interestingly, more signals were observed in those cells exposed to the highest concentration (100 μg/mL).

3.3. Cell viability in MH-S cells exposed to PETNPLs scored in sorted cells

To assess the potential cytotoxic effects of PETNPLs internalization, MH-S cells containing iDye-PETNPLs, were used. To proceed, positive MH-S cells were selected by sorting cells exposed to several concentrations (25, 50, and 100 μg/mL) for 24 h. As illustrated in Supplementary

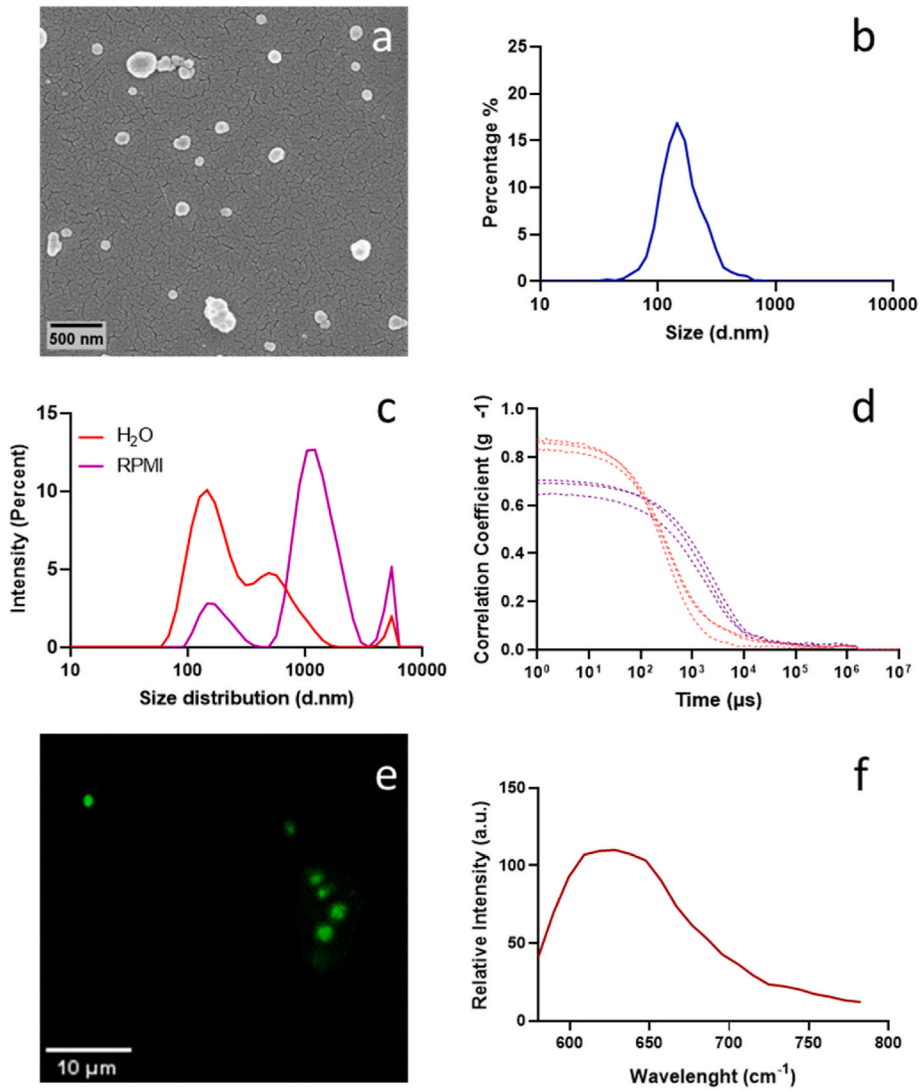

Fig. 1. (a) Characterization of PETNPLs morphology assessed by SEM. (b) Measured SEM size distribution of PETNPLs. (c) The intensity values for the hydrodynamic behavior of PETNPLS for both water (red) and media (purple) dispersion. (d) Correlation coefficients for (c) distribution data. (e, f) Visualization and fluorescent spectra confirmation for particle aggregates, as done by confocal microscopy and lambda scan, respectively. (For interpretation of the references to color in this figure legend, the reader is referred to the Web version of this article.)

Fig. S2 no significant changes in the viability of MH-S cells that uptake PETNPLs were observed. Therefore, no toxic effects are associated with the internalization of PETNPLs. This response is like that observed in overall exposed cell populations (unsorted ones). Thus, human leukemia monocytic THP-1 cells exposed to PETNPLs reported no significant decrease in cell viability after 24 h of exposure (Villacorta et al., 2022). However, that study chose the total exposed THP-1 cells to assess the cytotoxic response unlike we evaluated only the sub-populations of cells with PETNLs, as compared to total exposed cells, which may give a more precise and robust risk assessment of the effects. However, our data revealed that there was also no significant decrease in cell viability in only a subpopulation of cells with PETNPLs, as compared to the total population. This may add value to the existing information about the risk assessment of MNPLs. Moreover, the obtained data, along with other studies, may not only suggest the significance of cell viability that would aid in identifying the sub-lethal concentrations of the MNPLs but also its relevance to evaluating the subtle toxic effects like changes in ROS, MMP, and polarization of macrophages in only the cells containing PETNPLs; otherwise, these sub-toxic effects may be masked in the total exposed population. A recent study by Annangi et al. (2023) demonstrated the sub-lethal effects, like an increase in ROS and loss of MMP, due to PETNPLs in primary human nasal epithelial (HNEpCs) cells although they did not observe any significant decreases in cell viability at the tested concentrations (0–100 µg/mL). In accordance, no significant changes in cell viability were observed in three different human cell types [(human intestinal epithelial (Caco-2), human hepatoma (HepG2), and human hepatic (HepaRG) cells] after exposure to PE, PP, PET, and PVC MPLs (Stock et al., 2021) despite the successful internalization observed. This may escape the subtle or sub-lethal cellular effects in the exposed cells having the internalized MNPLs, thereby underestimating the risk posed by them.

Although this study utilized relatively high acute concentrations to assess the impacts of PETNPLs in the sorted cells, as compared to plausible environmentally relevant doses, a recent study estimated a significantly high mass of MPLs that could reach humans due to ingestion based on a meta-analysis of 59 research papers. It reported that humans may ingest 0.2–10 mg/day/kg for 70 kg man, which would translate to 0.1 to 5 per week (Senathirajah et al., 2021). Nevertheless, the extrapolation of the doses used here to possible real-life exposure conditions is out of the scope of this study.

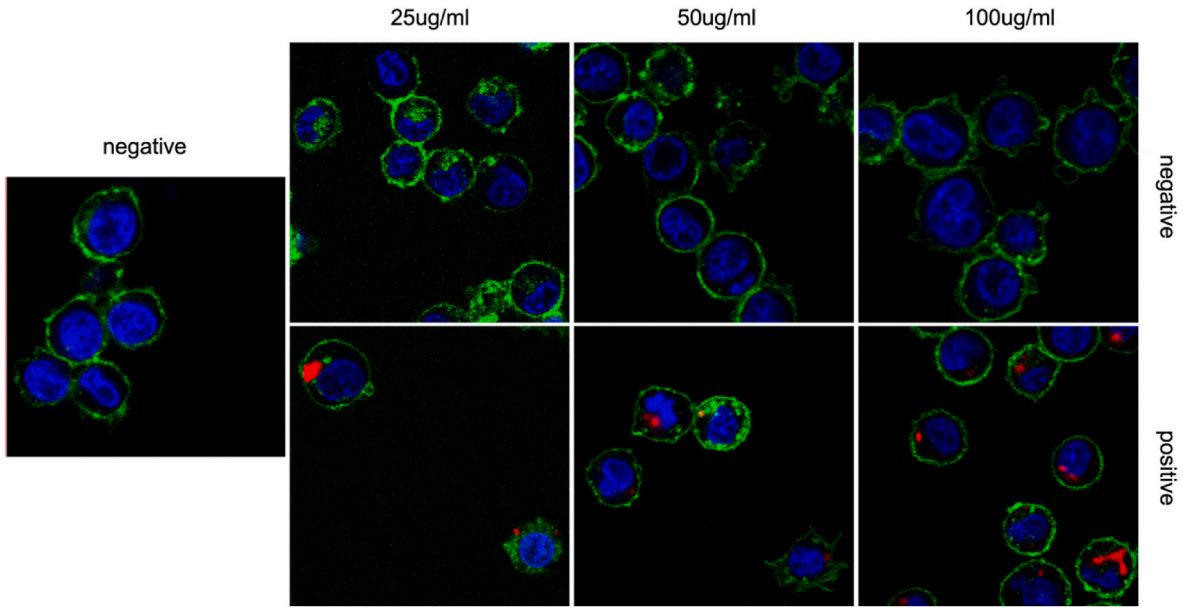

Fig. 2. Confocal microscopy images confirmed the presence of internalized PETNPLs in positive sorted MH-S cells. The red color represents the PETNPLs, and the green and blue colors represent the cell membrane and cell nuclei, respectively. No PETNPLs were observed neither in the negative sorted cells nor in the unexposed cells (0 μg/mL). (For interpretation of the references to color in this figure legend, the reader is referred to the Web version of this article.)

3.4. Induction of ROS by PETNPLs in gated cells

To achieve an insight into the harmful effects of exposure to PETNPLs, from a biological perspective, various biomarkers can be used. Among them, ROS is one of the crucial indicators to identify cellular stress and toxicity in response to external components. This biomarker is widely recognized in different studies where an imbalance in the antioxidant levels results in increased ROS production, leading to DNA damage and even to cellular death (Jomova et al., 2023). In this study, the intracellular oxidant levels in the gated cells having internalized PETNPLs at 3 and 24 h post-treatment were measured using the DCFH-DA assay. Specifically, our data indicated that PETNPLs would possibly elevate the oxidant levels, as compared with untreated cells, in a time-dependent manner (Fig. 3) through a redox signaling mechanism, since the DCFH probe utilized in this study might not measure H_2O_2 and other ROS levels, rather its oxidation could be catalyzed by iron ions (Fe^{+2}) in the presence of oxygen or H_2O_2 to DCF, the fluorescent subproduct. Furthermore, utilizing the probe might not result in a quantitative measurement of the generation of ROS (Kalyanaraman et al., 2012). Moreover, we found that there were significant increases in the oxidant levels only at the highest concentration tested (100 mg/mL) at 3 h post-treatment, but the oxidant levels after 24 h were significant at all the tested concentrations (Fig. 3). Previous studies suggested PETNPLs could generate ROS albeit with a varying degree in different cell types, a slight increase in ROS levels in mouse alveolar macrophages (RAW 246.7) (Aguilar-Guzmán et al., 2022), and similar weak effects were reported in human alveolar macrophages where increased ROS levels were only observed in one of the concentrations tested (Zhang et al., 2022), but there were obvious increases in production of ROS in human nasal epithelial cells exposed to PETNPLs (Annangi et al., 2023). It must be pointed out that all these studies have also utilized DCFH-DA as a probe which could estimate the oxidant levels over the generation of ROS (Kalyanaraman et al., 2012), hence the generation of ROS by PETNPLs may be not representative in the studies while employing DCFH probe for the estimation of ROS. Moreover, our study also addressed the biases associated with these studies considering they estimated the oxidant levels in the whole heterogenous population of cells exposed to PETNPLs, while the present study analyzed the oxidant levels in those gated cells having internalized PETNPLs, providing more robust data.

3.5. Loss of mitochondrial membrane potential in gated cells

The MMP is one of the indicators of cell toxicity (Sakamuru et al., 2016). Since mitochondria have been considered as a target of MNPL action (Cortés et al., 2020; Lin et al., 2022; Tavakolpournegari et al.,

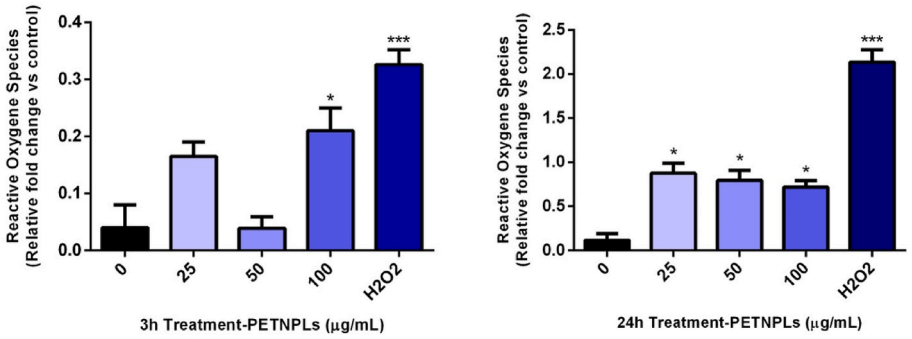

Fig. 3. The histograms show the fold change of ROS production in MH-S cells exposed to PETNPLs for 3 and 24 h at the concentrations of 0, 25, 50, and 100 μg/mL. Data are represented as mean ± SEM. $^{*}p < 0.05$, $^{***}p < 0.001$ (2-way ANOVA and Student's t-test).

2023), changes in MMP should be considered as a biomarker in those studies determining the potentially hazardous effects of MNPL exposure.

As observed in Fig. 4, our results revealed significant decreases in MMP values in those MH-S cells containing PETNPLs after exposures lasting for 24 h. These findings are in line with previous studies demonstrating the ability of PETNPLs to disrupt MMP in different cell lines, such as in adenocarcinoma human alveolar basal epithelial A549 cells (Zhang et al., 2022), and in human nasal epithelial primary (HNEpCs) cells (Annangi et al., 2023). Collectively, these studies underlined the consistent effect of PETNPLs on MMP in various cell types and reinforced the significance of our data in elucidating the specific consequences of PETNPL exposure on the MH-S cells that have internalized them. The mitochondrial membrane potential, in association with other toxic responses of cells, could show the harmful effect of environmental agents such as PETNPLs and, as discussed above, different cell types in the whole population of samples treated with MNPLs showed a significant change when assessed for the MMP. In this assay, we postulated that cells that internalized PETNPLs should show a remarkable change in MMP, concluding that PETNPLs can cause harmful effects on the mitochondria via MMP. It is important to point out the relevance of the exposure time on the expression of this biomarker. Accordingly, exposures lasting for 3 h were too short to induce the expected effects, which were observed when exposures were extended to 24 h.

3.6. Macrophage polarization by PETNPLs in gated cells

The macrophage response to environmental insults can appear as their polarization towards two distinct phenotypes called M1 and M2 that could act as pro-inflammatory and anti-inflammatory subtypes, respectively. This type of cellular response in macrophages could be a clue to identifying the immunotoxic effects of NPLs exposure in immune-based cells like MH-S cells (Pérez and Rius-Pérez, 2022; Wu et al., 2023).

In our study, the potential of PETNPLs in modulating the immune responses of mouse alveolar macrophages (MH-S cells) was evaluated by studying the toll-like receptors on the surface of the macrophages representing the polarized macrophage from M0 to M1 and M2 subtypes. The data indicated that the presence of PETNPLs in MH-S cells could significantly affect the polarization of the MH-S cells from M0 to M1 and M2 subtypes at exposures (0, 25, 50, and 100 μg/mL) lasting for 3 and 24 h. Interestingly, we observed a very significant polarization of macrophages (M0) towards the M1 subtype in the gated cells containing PETNPLs, as evidenced by the increased expression of the structural surface biomarker CD86. Its expression decreased when the concentration increased, in comparison with untreated cells at both exposure time points. This indicates the role of PETNPLs in eliciting a pro-inflammatory response (Fig. 5). Our results agree with the polarization towards a pro-inflammatory phenotype observed in MH-S cells exposed to PSNPLs when assessed by using the CD38 biomarker (Collin-Faure et al., 2022). Moreover, as indicated in Fig. 5, there was a consistent level of M0 to M1 polarization between the two time points lasting for 3–24 h, since this effect was significantly observed in the sorted cells with internalized PETNPLs at both time points. Hence, at different time points, the effects of PETNPLs to polarize the macrophages prominently to the M1 sub-type remained stable in the sorted cells with PETNPLs population. Unfortunately, no similar studies have been detected in the open literature to confirm the relevance of the exposure time, although the importance of time in macrophage polarization has been pointed out (Murray, 2017). Although without checking the presence of M1/M2 subtypes, indirect studies reporting the secretion of inflammatory cytokines in murine (RAW264.7) macrophages (Wang et al., 2023) and human lung macrophage cells (Washihira et al., 2023) after exposure to PS-MNPLs exposure suggest a role on macrophage polarization. Furthermore, a study using different NPLs with different sizes displayed strongly modulated cytokine secretion patterns, suggesting downregulation of the inflammatory phenotype indicative of M2 macrophage induction, and more towards a pro-inflammatory phenotype i.e. M1 sub-type (Wolff et al., 2023).

Besides, our data also revealed that there was a polarizing effect towards the M2 subtype in the gated cells containing PETNPLs, as observed by the increased expression of CD163 surface biomarker when compared to the untreated cells. These effects were more evident after 24 h of treatment at all concentrations tested suggesting the existence of a subpopulation of macrophages (M2) in the total population involved in anti-inflammatory or wound-healing responses with the M1 subtype. The response behind the different M2 responses between 3 and 24 h of exposure might agree with the macrophage immune response toward the time; meaning that at the very beginning of recognizing external insults, the immune pro-inflammatory response of macrophages occurs, while later, and to reduce the effects of pro-inflammatory cytokines, the M2 phenotype of the macrophages would raise and neutralize the pro-inflammation outcomes (Murray, 2017). Similarly, an M2 polarization of rainbow trout macrophages (RT-HKM) exposed to PSNPLs was reported, inferring an anti-inflammatory response in these cells (Brandts et al., 2023), as well as observed in macrophages derived from human monocytes (Wolff et al., 2023). It is important to point out that using true-to-life PETMPLs in an *in vivo* mouse model, a recent study including RNA-seq analysis has demonstrated that exposure affects immune homeostasis (Harusato et al., 2023).

To complement the previous FC studies, the potential macrophage polarization resulting from PETNPL exposure was assessed by immunocytochemistry using confocal microscopy. As a complementary study, this approach was only performed by detecting CD86 in the cell membrane. The obtained data showed that the cells containing PETNPLs triggered a macrophagic polarization from M0 to M1 (CD86) subtype because of PETNPLs internalization at 100 μg/mL concentration after

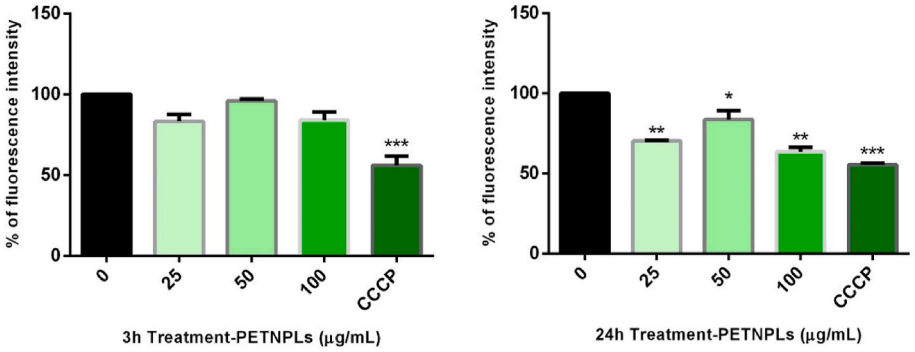

Fig. 4. The histograms show the effects of PETNPLs on the mitochondrial membrane potential of gated MH-S cells exposed for 3 and 24 h. The exposure lasting for 24 h resulted in a significant decrease in the mitochondrial membrane potential, in comparison with the lack of effect of exposures lasting for 3 h. Data are represented as mean ± SEM. *$p < 0.05$, **$p < 0.01$, ***$p < 0.001$ (2-way ANOVA and Student's t-test).

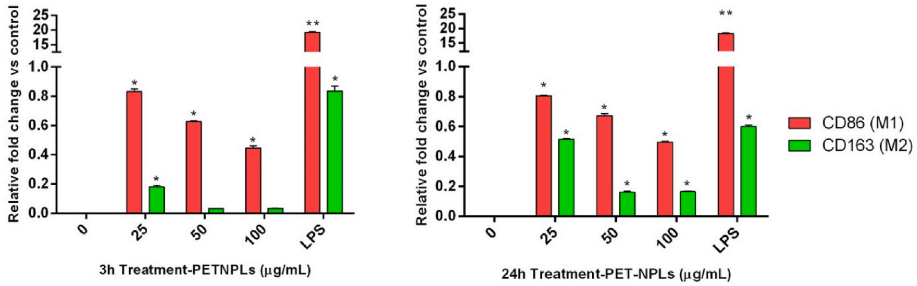

Fig. 5. The histograms indicate the influence of PETNPLs on the macrophage polarization from M0 to M1 and M2 subtypes in exposed MH-S cells. Data are represented as mean ± SEM. $*p < 0.05$, $**p < 0.01$, (2-way ANOVA and Student's t-test).

24 h of exposure (Fig. 6, a2).

From a global comprehensive point of view, the results describe the interconnection between MMP, ROS, and the immune response to PETNPL exposures. Alterations in MMP and ROS, not only are related to each other because the mitochondrial membrane potential acts as the main source of the intracellular ROS (Suski et al., 2018), but also considering the pathological issues caused by alterations in ROS and MMP balance that produce an inflammatory response. This idea is clear in the current study in a way that by looking at the obtained data, the harmonic trend between MMP, ROS, and M1/M2 macrophage polarization, even between the times of exposure and the concentrations, shows the connective outcome, as explained in the study of Wang et al. (2021) were changes in the mitochondrial membrane potential and the oxidative stress affected the regulation and activation of macrophage and immune system via different pathways.

The mitochondrial metabolism and the physiology of macrophages can be affected by different environmental factors and stimuli, which allow to polarize of the macrophages into pro-inflammatory M1 phenotype or anti-inflammatory M2 phenotype (Xu et al., 2022). Mitochondrial dysfunction such as loss of MMP may reprogram the energy metabolism as a decrease in mitochondrial oxidative metabolism, elevated uptake of glucose, and its breakdown *via* glycolysis (Bao et al., 2021). All this may lead to nitric oxide (NO) mediated accumulation of ROS which might prevent repolarization of M1 to M2 macrophages, skewing towards an inflammatory response (Bedard and Krause, 2007). However, by restoring the mitochondrial function the response from inflammatory to anti-inflammatory macrophages could be reversed (Van den Bossche et al., 2016).

4. Conclusion

The increasing levels of environmental plastic waste pollution require urgent studies to determine their potential toxicological profile, particularly regarding the byproducts resulting from their degradation (MNPLs). Since inhalation is an important exposure route to MNPLs, we have used mouse alveolar macrophages (MH-S) as an appropriate target. Aiming to evaluate representative MNPLs, we have used true-to-life PETNPLs obtained by sanding PET water bottles as an approach to those secondary MNPLs present in the environment. Finally, to pick up biomarkers with potential health implications, we have focused on assessing the toxic and immunotoxic effects of the selected PETNPLs. As a first conclusion, we have shown that MH-S cells efficiently internalize PETNPLs, with a 100% internalization at the concentration of 100 μg/mL. Our findings unequivocally demonstrate the harmful impact of PETNPLs on macrophage functions. This impact is evident through the disruption of the mitochondrial function, the elevated intracellular ROS levels, and the significant alterations in macrophage polarization, shifting the balance between M1 and M2 phenotypes. Due to the health relevance of the described biomarkers, our results underscore the need for further research, particularly focusing on factors such as NPL types, selected biomarkers, and cell types, to better understand the health implications associated with MNPL exposure. In addition to evaluating other MNPLs, other representative cell lung types such as the Calu-3 cells derived from human non-small-cell lung adenocarcinoma epithelial cells should be used. The advantage of this cell line is that can be used for the establishment of an *in vitro* lung epithelium barrier model since can display epithelial morphology expressing tight junctions and secreting abundant mucous substances. In addition, this cell line presents long-term stability which permits determining both acute and long-term effects. In such a model, other relevant biomarkers should be included i.e., genotoxicity. It must be stated that genotoxicity has become an indispensable biomarker in any hazard evaluation. It is well known that DNA damage can drive very relevant health consequences such as gene/chromosome mutation, carcinogenesis, and aging, among others but,

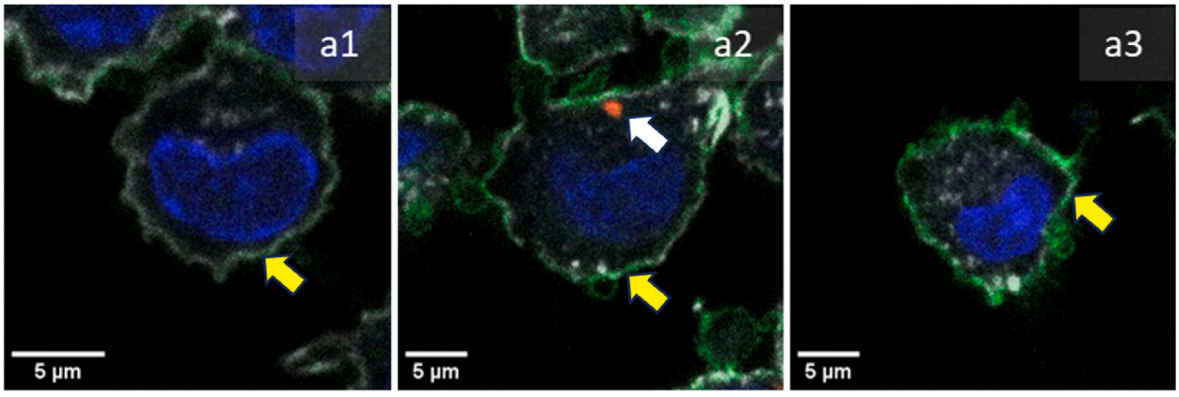

Fig. 6. MH-S cells were analyzed by confocal microscopy to detect CD86, as a surface marker of the M1 macrophage stage. (a1) Untreated control, (a2) cells with PETNPLs, and (a3) positive control cells exposed to LPS. The red spot indicates the internalized PETNPLs (white arrow), blue and gray colors are cell nuclei and actin, respectively. The green color indicates the expression of CD86 on the surface of the MH-S cells (a2 and a3), pointed out with yellow arrows. (For interpretation of the references to color in this figure legend, the reader is referred to the Web version of this article.)

despite the relevance of this biomarker, very few studies have evaluated the potential genotoxic effects of MNPLs (Tagorti and Kaya, 2022).

CRediT authorship contribution statement

Alireza Tavakolpournegari: Investigation. **Aliro Villacorta:** Methodology. **Michelle Morataya-Reyes:** Methodology. **Jéssica Arribas Arranz:** Investigation. **Gooya Banaei:** Investigation. **Susana Pastor:** Investigation, Data curation. **Antonia Velázquez:** Validation, Investigation. **Ricard Marcos:** Writing – review & editing, Supervision, Conceptualization. **Alba Hernández:** Writing – review & editing, Funding acquisition, Conceptualization. **Balasubramanyam Annangi:** Writing – review & editing, Writing – original draft, Supervision, Conceptualization.

Declaration of competing interest

The authors declare that they have no known competing financial interests or personal relationships that could have appeared to influence the work reported in this paper.

Data availability

Data will be made available on request.

Acknowledgments

AT and MMR hold Ph.D. fellowships from the Generalitat de Catalunya. AV was supported by a Ph.D. fellowship from the National Agency for Research and Development (ANID), CONICYT PFCHA/DOCTORADO BECAS CHILE/2020–72210237. AH was granted an ICREA ACADEMIA award.

This project (Plasticheal) has received funding from the European Union's Horizon 2020 research and innovation programme under grant agreement No 965196. This work was also partially supported by the Spanish Ministry of Science and Innovation [PID2020-116789, RB-C43] and by the Generalitat de Catalunya (2021-SGR-00731).

Appendix A. Supplementary data

Supplementary data to this article can be found online at https://doi.org/10.1016/j.envpol.2024.123823.

References

Aguilar-Guzmán, J.C., Bejtka, K., Fontana, M., Valsami-Jones, E., Villezcas, A.M., Vazquez-Duhal, R., Rodríguez-Hernámdez, A.G., 2022. Polyethylene terephthalate nanoparticles effect on RAW 264.7 macrophage cells. Micropl. Nanopl. 2, 9. https://doi.org/10.1186/s43591-022-00027-1.

Allard, B., Panariti, A., Martin, J.G., 2018. Alveolar macrophages in the resolution of inflammation, tissue repair, and tolerance to infection. Front. Immunol. 9, 1777. https://doi.org/10.3389/fimmu.2018.01777.

Annangi, B., Villacorta, A., Vela, L., Tavakolpournegari, A., Marcos, R., Hernández, A., 2023. Effects of true-to-life PET nanoplastics using primary human nasal epithelial cells. Environ. Toxicol. Pharmacol. 100, 104140 https://doi.org/10.1016/j.etap.2023.104140.

Bao, X., Zhang, J., Huang, G., Yan, J., Xu, C., Dou, Z., Sun, C., Zhang, H., 2021. The crosstalk between HIFs and mitochondrial dysfunctions in cancer development. Cell Death Dis. 12 (2), 215. https://doi.org/10.1038/s41419-021-03505-1.

Bedard, K., Krause, K.H., 2007. The NOX family of ROS-generating NADPH oxidases: physiology and pathophysiology. Physiol. Rev. 87 (1), 245–313. https://doi.org/10.1152/physrev.00044.2005.

Bhutto, S.U.A., Ma, Y.F., Akram, M., You, X.Y., 2023. Microplastics in Tai lake food web: trophic transfer and human health risk assessment. Environ. Toxicol. Pharmacol. 101, 104206 https://doi.org/10.1016/j.etap.2023.104206.

Brandts, I., Solà, R., Garcia-Ordoñez, M., Gella, A., Quintana, A., Martin, B., Esteve-Codina, A., Teles, M., Roher, N., 2023. Polystyrene nanoplastics target lysosomes interfering with lipid metabolism through the PPAR system and affecting macrophage functionalization. Environ. Sci.: Nano 10, 2245–2258. https://doi.org/10.1039/D2EN01077A.

Carbery, M., O'Connor, W., Palanisami, T., 2018. Trophic transfer of microplastics and mixed contaminants in the marine food web and implications for human health. Environ. Int. 115, 400–409. https://doi.org/10.1016/j.envint.2018.03.007.

Chen, Q., Gao, J., Yu, H., Su, H., Yang, Y., Cao, Y., Zhang, Q., Ren, Y., Hollert, H., Si, H., Chen, C., Liu, H., 2022. An emerging role of microplastics in the etiology of lung ground glass nodules. Environ. Sci. Eur. 34 (1), 25. https://doi.org/10.1186/s12302-022-00605-3.

Ciaglia, E., Montella, F., Trucillo, P., Ciardulli, M.C., Di Pietro, P., Amodio, G., Remondelli, P., Vecchione, C., Reverchon, E., Maffulli, N., Puca, A.A., Della Porta, G., 2019. A bioavailability study on microbeads and nanoliposomes fabricated by dense carbon dioxide technologies using human-primary monocytes and flow cytometry assay. Int. J. Pharm. 570, 118686 https://doi.org/10.1016/j.ijpharm.2019.118686.

Collin-Faure, V., Dalzon, B., Devcic, J., Diemer, H., Cianférani, S., Rabilloud, T., 2022. Does size matter? A proteomics-informed comparison of the effects of polystyrene beads of different sizes on macrophages. Environ. Sci.: Nano 9, 2827–2840. https://doi.org/10.1039/d2en00214k.

Cortés, C., Domenech, J., Salazar, M., Pastor, S., Marcos, R., Hernández, H., 2020. Nanoplastics as potential environmental health factors. Effects of polystyrene nanoparticles on the human intestinal epithelial Caco-2 cells. Environ. Sci.: Nano 7, 272–285. https://doi.org/10.1039/c9en00523d.

Delaney, S., Rodriguez, C., Sarrett, S.M., Dayts, E.J., Zeglis, B.M., Keinänen, O., 2023. Unraveling the *in vivo* fate of inhaled micro- and nanoplastics with PET imaging. Sci. Total Environ. 904, 166320 https://doi.org/10.1016/j.scitotenv.2023.166320.

Deng, J., Ibrahim, M.S., Tan, L.Y., Yeo, X.Y., Lee, Y.A., Park, S.J., Wüstefeld, T., Park, J. W., Jung, S., Cho, N.J., 2022. Microplastics released from food containers can suppress lysosomal activity in mouse macrophages. J. Hazard Mater. 435, 128980 https://doi.org/10.1016/j.jhazmat.2022.128980.

Domenech, J., Hernández, A., Demir, E., Marcos, R., Cortés, C., 2020. Interactions of graphene oxide and graphene nanoplatelets with the *in vitro* Caco-2/HT29 model of the intestinal barrier. Sci. Rep. 10 (1), 2793. https://doi.org/10.1038/s41598-020-59755-0.

Fuchs, A.K., Syrovets, T., Haas, K.A., Loos, C., Musyanovych, A., Mailänder, V., Landfester, K., Simmet, T., 2016. Carboxyl- and amino-functionalized polystyrene nanoparticles differentially affect the polarization profile of M1 and M2 macrophage subsets. Biomaterials 85, 78–87. https://doi.org/10.1016/j.biomaterials.2016.01.064.

Gigault, J., El Hadri, H., Nguyen, B., Grassl, B., Rowenczyk, L., Tufenkji, N., Feng, S., Wiesner, M., 2021. Nanoplastics are neither microplastics nor engineered nanoparticles. Nat. Nanotechnol. 16 (5), 501–507. https://doi.org/10.1038/s41565-021-00886-4.

Harusato, A., Seo, W., Abo, H., Nakanishi, Y., Nishikawa, H., Itoh, Y., 2023. Impact of particulate microplastics generated from polyethylene terephthalate on gut pathology and immune microenvironments. iScience 26 (4), 106474. https://doi.org/10.1016/j.isci.2023.106474.

Jenner, L.C., Rotchell, J.M., Bennett, R.T., Cowen, M., Tentzeris, V., Sadofsky, L.R., 2022. Detection of microplastics in human lung tissue using μFTIR spectroscopy. Sci. Total Environ. 831, 154907 https://doi.org/10.1016/j.scitotenv.2022.154907.

Jomova, K., Raptova, R., Alomar, S.Y., Alwasel, S.H., Nepovimova, E., Kuca, K., Valko, M., 2023. Reactive oxygen species, toxicity, oxidative stress, and antioxidants: chronic diseases and aging. Arch. Toxicol. 97 (10), 2499–2574. https://doi.org/10.1007/s00204-023-03562-9.

Kalyanaraman, B., Darley-Usmar, V., Davies, K.J., Dennery, P.A., Forman, H.J., Grisham, M.B., Mann, G.E., Moore, K., Roberts, L.J., Ischiropoulos, H., 2012. Measuring reactive oxygen and nitrogen species with fluorescent probes: challenges and limitations. Free Rad. Biol. Med. 52 (1), 1–6. https://doi.org/10.1016/j.freeradbiomed.2011.09.030.

Karakolis, E.G., Nguyen, B., You, J.B., Rochman, C.M., Sinton, D., 2019. Fluorescent dyes for visualizing microplastic particles and fibers in laboratory-based studies. Environ. Sci. Technol. Lett. 6 (6), 334–340. https://doi.org/10.1021/acs.estlett.9b00241.

Kim, L., Cui, R., Il Kwak, J., An, Y.J., 2022. Trophic transfer of nanoplastics through a microalgae-crustacean-small yellow croaker food chain: inhibition of digestive enzyme activity in fish. J. Hazard Mater. 440, 129715 https://doi.org/10.1016/j.jhazmat.2022.129715.

Koner, K., Florance, I., Mukherjee, A., Chandrasekaran, N., 2023. Cellular response of THP-1 macrophages to polystyrene microplastics exposure. Toxicology 483, 153385. https://doi.org/10.1016/j.tox.2022.153385.

Kumar, R., Manna, C., Padha, S., Verma, A., Sharma, P., Dhar, A., Ghosh, A., Bhattacharya, P., 2022. Micro(nano)plastics pollution and human health: How plastics can induce carcinogenesis to humans? Chemosphere 298, 134267. https://doi.org/10.1016/j.chemosphere.2022.134267.

Latroche, C., Weiss-Gayet, M., Gitiaux, C., Chazaud, B., 2018. Cell sorting of various cell types from mouse and human skeletal muscle. Methods 134–135, 50–55. https://doi.org/10.1016/j.ymeth.2017.12.013.

Le, V.G., Nguyen, M.K., Nguyen, H.L., Lin, C., Hadi, M., Hung, N.T.Q., Hoang, H.G., Nguyen, K.N., Tran, H.T., Hou, D., Zhang, T., Bolan, N.S., 2023. A comprehensive review of micro- and nano-plastics in the atmosphere: occurrence, fate, toxicity, and strategies for risk reduction. Sci. Total Environ. 904, 166649 https://doi.org/10.1016/j.scitotenv.2023.166649.

Lim, D., Jeong, J., Song, K.S., Sung, J.H., Oh, S.M., Choi, J., 2021. Inhalation toxicity of polystyrene micro(nano)plastics using modified OECD TG 412. Chemosphere 262, 128330. https://doi.org/10.1016/j.chemosphere.2020.128330.

Lin, S., Zhang, H., Wang, C., Su, X.L., Song, Y., Wu, P., Yang, Z., Wong, M.H., Cai, Z., Zheng, C., 2022. Metabolomics reveal nanoplastic-induced mitochondrial damage in human liver and lung cells. Environ. Sci. Technol. 56 (17), 12483–12493. https://doi.org/10.1021/acs.est.2c03980.

Murray, P.J., 2017. Macrophage polarization. Annu. Rev. Physiol. 79, 541–566. https://doi.org/10.1146/annurev-physiol-022516-034339.

Nanogenotox project, 2011. Final protocol for producing suitable manufactured nanomaterial exposure media. Nanogenotox, towards a method for detecting the potential genotoxicity of nanomaterials. https://www.anses.fr/en/system/files/nanogenotox_deliverable_5.pdf. (Accessed 15 June 2023).

Nguyen, B., Tufenkji, N., 2022. Single-particle resolution fluorescence microscopy of nanoplastics. Environ. Sci. Technol. 56 (10), 6426–6435. https://doi.org/10.1021/acs.est.1c08480.

Pérez, S., Rius-Pérez, S., 2022. Macrophage polarization and reprogramming in acute inflammation: a redox perspective. Antioxidants 11 (7), 1394. https://doi.org/10.3390/antiox11071394.

Pulvirenti, E., Ferrante, M., Barbera, N., Favara, C., Aquilia, E., Palella, M., Cristaldi, A., Conti, G.O., Fiore, M., 2022. Effects of nano and microplastics on the inflammatory process: *in vitro* and *in vivo* studies systematic review. Front. Biosci. 27 (10), 287. https://doi.org/10.31083/j.fbl2710287.

Rubio, L., Marcos, R., Hernández, A., 2020. Potential adverse health effects of ingested micro- and nanoplastics on humans. Lessons learned from *in vivo* and *in vitro* mammalian models. J. Toxicol. Environ. Health B Crit. Rev. 23 (2), 51–68. https://doi.org/10.1080/10937404.2019.1700598.

Sakamuru, S., Attene-Ramos, M.S., Xia, M., 2016. Mitochondrial membrane potential assay. Methods Mol. Biol. 1473, 17–22. https://doi.org/10.1007/978-1-4939-6346-1_2.

Senathirajah, K., Attwood, S., Bhagwat, G., Carbery, M., Wilson, S., Palanisami, T., 2021. Estimation of the mass of microplastics ingested - a pivotal first step towards human health risk assessment. J. Hazard Mater. 404 (Pt B), 124004 https://doi.org/10.1016/j.jhazmat.2020.124004.

Stock, V., Laurisch, C., Franke, J., Dönmez, M.H., Voss, L., Böhmert, L., Braeuning, A., Sieg, H., 2021. Uptake and cellular effects of PE, PP, PET, and PVC microplastic particles. Toxicol. Vitro 70, 105021. https://doi.org/10.1016/j.tiv.2020.105021.

Suski, J., Lebiedzinska, M., Bonora, M., Pinton, P., Duszynski, J., Wieckowski, M.R., 2018. Relation between mitochondrial membrane potential and ROS formation. Methods Mol. Biol. 1782, 357–381. https://doi.org/10.1007/978-1-4939-7831-1_22.

Tagorti, G., Kaya, B., 2022. Genotoxic effect of microplastics and COVID-19: the hidden threat. Chemosphere 286 (Pt 3), 131898. https://doi.org/10.1016/j.chemosphere.2021.131898.

Tavakolpournegari, A., Annangi, B., Villacorta, A., Banaei, G., Martin, J., Pastor, S., Marcos, R., Hernández, A., 2023. Hazard assessment of different-sized polystyrene nanoplastics in three hematopoietic human cell lines. Chemosphere 325, 138360. https://doi.org/10.1016/j.chemosphere.2023.138360.

Tursi, A., Baratta, M., Easton, T., Chatzisymeon, E., Chidichimo, F., De Biase, M., De, Filpo G., 2022. Microplastics in aquatic systems, a comprehensive review: origination, accumulation, impact, and removal technologies. RSC Adv. 12 (44), 28318–28340. https://doi.org/10.1039/d2ra04713f.

Van den Bossche, J., Baardman, J., Otto, N.A., van der Velden, S., Neele, A.E., van den Berg, S.M., Luque-Martin, R., Chen, H.J., Boshuizen, M.C., Ahmed, M., Hoeksema, M.A., de Vos, A.F., de Winther, M.P., 2016. Mitochondrial dysfunction prevents repolarization of inflammatory macrophages. Cell Rep. 17 (3), 684–696. https://doi.org/10.1016/j.celrep.2016.09.008.

Villacorta, A., Rubio, L., Alaraby, M., López-Mesas, M., Fuentes-Cebrian, V., Moriones, O. H., Marcos, R., Hernández, A., 2022. A new source of representative secondary PET nanoplastics. Obtention, characterization, and hazard evaluation. J. Hazard Mater. 439, 129593 https://doi.org/10.1016/j.jhazmat.2022.129593.

Villacorta, A., Vela, L., Morataya-Reyes, M., Llorens-Chiralt, R., Rubio, L., Alaraby, M., Marcos, R., Hernández, A., 2023. Titanium-doped PET nanoplastics of environmental origin as a true-to-life model of nanoplastic. Sci. Total Environ. 880, 163151 https://doi.org/10.1016/j.scitotenv.163151.

Wang, Y., Li, N., Zhang, X., Horng, T., 2021. Mitochondrial metabolism regulates macrophage biology. J. Biol. Chem. 297 (1), 100904 https://doi.org/10.1016/j.jbc.2021.100904.

Wang, X., Ren, X.M., He, H., Li, F., Liu, K., Zhao, F., Hu, H., Zhang, P., Huang, B., Pan, X., 2023. Cytotoxicity and pro-inflammatory effect of polystyrene nano-plastic and micro-plastic on RAW264.7 cells. Toxicology 484, 153391. https://doi.org/10.1016/j.tox.2022.153391.

Washihira, N., Murakami, M., Nakamura, M., Fujii, S., Matsushima, T., Asahara, H., Kishida, A., Tanabe, T., Kimura, T., Kobayashi, M., Yamamoto, M., 2023. Application of a genetically engineered macrophage cell line for evaluating cellular effects of UV/US-treated poly (ethylene terephthalate) microplastics. Colloids Surf. B Biointerfaces 234, 113735. https://doi.org/10.1016/j.colsurfb.2023.113735.

Wolff, C.M., Singer, D., Schmidt, A., Bekeschus, S., 2023. Immune and inflammatory responses of human macrophages, dendritic cells, and T-cells in presence of micro- and nanoplastic of different types and sizes. J. Hazard Mater. 459, 132194 https://doi.org/10.1016/j.jhazmat.2023.132194.

Wu, Y., Yao, Y., Bai, H., Shimizu, K., Li, R., Zhang, C., 2023. Investigation of pulmonary toxicity evaluation on mice exposed to polystyrene nanoplastics: the potential protective role of the antioxidant N-acetylcysteine. Sci. Total Environ. 855, 158851.

Xu, L., Yan, X., Zhao, Y., Wang, J., Liu, B., Yu, S., Fu, J., Liu, Y., Su, J., 2022. Macrophage polarization mediated by mitochondrial dysfunction induces adipose tissue inflammation in obesity. Int. J. Mol. Sci. 23 (16), 9252.

Yang, S., Cheng, Y., Chen, Z., Liu, T., Yin, L., Pu, Y., Liang, G., 2021. In vitro evaluation of nanoplastics using human lung epithelial cells, microarray analysis and co-culture model. Ecotoxicol. Environ. Saf. 226, 112837 https://doi.org/10.1016/j.ecoenv.2021.112837.

Zhang, H., Zhang, S., Duan, Z., Wang, L., 2022. Pulmonary toxicology assessment of polyethylene terephthalate nanoplastic particles *in vitro*. Environ. Int. 162, 107177 https://doi.org/10.1016/j.envint.2022.107177.

Zingaro, F., Gianoncelli, A., Ceccone, G., Birarda, G., Cassano, D., La Spina, R., Agostinis, C., Bonanni, V., Ricci, G., Pascolo, L., 2023. Morphological and lipid metabolism alterations in macrophages exposed to model environmental nanoplastics traced by high-resolution synchrotron techniques. Front. Immunol. 14, 1247747 https://doi.org/10.3389/fimmu.2023.1247747.

Update

Environmental Pollution

Volume 349, Issue , 15 May 2024, Page

DOI: https://doi.org/10.1016/j.envpol.2024.123996

Environmental Pollution 349 (2024) 123996

Contents lists available at ScienceDirect

Environmental Pollution

journal homepage: www.elsevier.com/locate/envpol

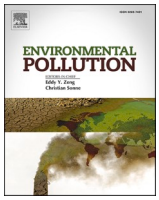

Corrigendum to "Harmful effects of true-to-life nanoplastics derived from PET water bottles in human alveolar macrophages" [Environ. Pollut., **348**: 123823 (2024)]

A. Tavakolpournegari, A. Villacorta, M. Morataya-Reyes, J. Arribas Arranz, G. Banaei, S. Pastor, A. Velázquez, R. Marcos *, A. Hernández, B. Annangi

Universitat Autònoma de Barcelona, Spain

The authors regret the presence of the word "human" in the title. The correct word is "mouse".

The authors would like to apologise for any inconvenience caused.

DOI of original article: https://doi.org/10.1016/j.envpol.2024.123823.

* Corresponding author.
E-mail address: ricard.marcos@uab.es (R. Marcos).

https://doi.org/10.1016/j.envpol.2024.123996

Available online 18 April 2024